Conference materials
UDC УДК 539.213.2:539.25
DOI: https://doi.org/10.18721/JPM.153.126

Effect of high-speed nonequilibrium on morphological and magnetic properties of melt-spun $Co_{58}Ni_{10}Fe_5Si_{11}B_{16}$ alloy

A. M. Frolov [1] ✉, T. A. Pisarenko [2], G. S. Kraynova [1], N. V. Ilin [1], A. Yu. Ralin [1]

[1] Far Eastern Federal University, Vladivostok, Russia;

[2] Institute of Automation and Control Processes Far Eastern Branch of the RAS, Vladivostok, Russia

✉ froloff5@yandex.ru

Abstract: The work presents a study on the influence of high-speed nonequilibrium of the melt-spinning process on the morphological and magnetic properties of the amorphous $Co_{58}Ni_{10}Fe_5Si_{11}B_{16}$ alloy. It is shown that the amorphous states with a different extent of disordering may be produced by varying the melt-spinning conditions. A correlation has been established between the fractal structure of morphological inhomogeneities and the magnetic properties of the melt-spun alloy: the higher the fractal dimension of the hierarchical mesoscale structure, the more the soft magnetic alloy. The optimal ordering of both the morphological and magnetic structure of the melt-spun Co58Ni10Fe5Si11B16 alloy is achieved at a cooling roller speed of 28 m/s.

Keywords: melt-spun alloy, morphology, mesoscale defects, fractal dimension, magnetism, coercitivity

Funding: The work was supported by State Task of the Ministry of Science and Higher Education of the Russian Federation under Grant no. 0657-2020-0005.

Citation: Frolov A. M., Pisarenko T.A., Kraynova G. S., Ilin N. V., Ralin A. Yu., Effect of high-speed nonequilibrium on morphological and magnetic properties of melt-spun $Co_{58}Ni_{10}Fe_5Si_{11}B_{16}$ alloy, St. Petersburg State Polytechnical University Journal. Physics and Mathematics. 15 (3.1) (2022) 155–161. DOI: https://doi.org/10.18721/JPM.153.126

Материалы конференции
УДК 539.213.2:539.25
DOI: https://doi.org/10.18721/JPM.153.126

Влияние высоко-скоростной неравновесности на структурно-морфологические и магнитные свойства быстрозакаленного сплава $Co_{58}Ni_{10}Fe_5Si_{11}B_{16}$

А. М. Фролов [1] ✉, Т. А. Писаренко [2], Г. С. Крайнова [1], Н. В. Ильин [1], А. Ю. Ралин [1]

[1] Дальневосточный Федеральный Университет, г. Владивосток, Россия;

[2] Институт автоматики и процессов управления Дальневосточного отделения РАН, г. Владивосток, Россия;

✉ froloff5@yandex.ru

Аннотация. В работе представлены результаты исследования морфологии и магнитных свойств сплава $Co_{58}Ni_{10}Fe_5Si_{11}B_{16}$ в зависимости от скоростных режимов получения. Показано, что технология спиннингования при вариации параметров получения позволяет получить аморфные состояния с разной степенью разупорядочения. В ходе работы установлена корреляция фрактальной структуры морфонеоднородностей и магнитных свойств быстрозакаленных сплавов: чем выше фрактальная размерность иерархической мезомасштабной структуры, тем более ярко выражены магнитомягкие свойства. Оптимальное упорядочение как морфологической, так и магнитной структуры сплава $Co_{58}Ni_{10}Fe_5Si_{11}B_{16}$ достигается при скорости роллера 28 м/с.

Ключевые слова: быстрозакаленный сплав, морфология, мезомасштабные дефекты, фрактальная размерность, магнетизм, коэрцитивность

Финансирование: Исследование выполнено при поддержке гранта Минобрнауки РФ № 0657-2020-0005.

Ссылка при цитировании: Фролов А. М., Писаренко Т. А., Крайнова Г. С., Ильин Н. В., Ралин А. Ю. Влияние высоко-скоростной неравновесности на структурно-морфологические и магнитные свойства быстрозакаленного сплава $Co_{58}Ni_{10}Fe_5Si_{11}B_{16}$ // Научно-технические ведомости СПбГПУ. Физико-математические науки. 2022. Т. 15. № 3.1. С. 155–161. DOI: https://doi.org/10.18721/JPM.123.126

Introduction

Amorphous metal alloys (AMA) are of great scientific interest in the study of the physical properties of disordered system. Soft magnetic AMA fabricated by the melt-spinning technique has a high magnetic permeability as a result one may be successfully applied for the manufacture of magnetic heads, magnetic shields, and secondary power supplies [1–4]. These alloys have high strength and corrosion resistance, which is important for operation in aggressive environments.

In order to increase the practical efficiency of such materials in technology, it is necessary to find new ways to control their special properties. For this reason, there has recently been an increased interest in studying the structural state and functional properties of melt-spun alloys, in particular, those made of soft magnetic materials.

The goal of this study is to identify the structural/morphological ordering and magnetic ordering in cobalt-based AMA produced by melt-spinning on a cooling roller at various technological conditions. It is interesting to study the correlations of the surface morphology and physical properties with a change in high-speed nonequilibrium, since, on the one hand, disordered media are characterized by the collective behavior of defects forming a hierarchical system with a fractal structure in the configuration space [5–7], and, on the other hand, it is well known that magnetic properties are structure-sensitive [4, 8, 9].

Materials and Methods

Amorphous $Co_{58}Ni_{10}Fe_5Si_{11}B_{16}$ alloys were fabricated by the melt-spinning technique with a single Cu roller at various linear speeds on the MeltSpinner SC equipment. Several samples of ribbons from this alloy were prepared, parametrized by high-speed production conditions. Technological and geometric parameters of the ribbons are given in Table 1.

Table 1

Parameters of samples

Sample	V, m/s	P_1, mbar	P_2, mbar	t, mm
A	22.0±0.1	50±5	200±5	21.0±4
B	25.1±0.1	50±5	250±5	23.0±1
C	28.3±0.1	50±5	350±5	23.0±1
D	31.4±0.1	50±5	350±5	19.3±0.5
E	37.0±0.1	60±5	400±5	16.0 ±1

Notations. *V* is the linear speed of the cooling roller, P_1 is the pressure in the chamber, P_2 is the pressure in the crucible, *t* is the ribbon thickness.

As seen from Table 1, in this series of samples, the cooling roller speed (*V*) is the most interesting parameter which affects the nonequilibrium of the melt-spinning process. In addition, it should be noted that at low P_1, with an increase of the linear speed of the cooling roller, an increase of P_2 is necessary to maintain the ribbon thickness.

To identify the atomic ordering, we used the X-ray diffraction method by a Bruker D8 Advance diffractometer, Fe-K_α radiation.

Morphology analysis was carried out using amorphous alloy HRTEM images obtained on FEI TITAN 300 TEM. The samples were preliminarily prepared: 3 mm circles were cut from the ribbon bulk, which were then placed in an ionic thinning plant (GATAN PIPS Model 691), where they were thinned until through holes appeared in central part.

Fraunhofer diffraction patterns were obtained by the System for Spectral Analysis of Electron-Optical Imaging software for digital spectral analysis of images, based on the FFT procedure [10]. The spectrum of spatial inhomogeneities (integral frequency characteristic) was calculated as a result of angular convolution of Fraunhofer diffraction pattern. Moreover, HRTEM images were parametrized by fractal dimensions using the fracton technique for analyzing a structural ordering based on the integral frequency characteristic [7].

Hysteresis loops and magnetization curves for the $Co_{58}Ni_{10}Fe_5Si_{11}B_{16}$ alloy were measured on an automated vibromagnetometer.

Results and Discussion

X-ray diffraction analysis showed that the melt-spun $Co_{58}Ni_{10}Fe_5Si_{11}B_{16}$ alloy remains X-ray amorphous at all speed conditions [11], and the profiles of X-ray diffraction patterns practically coincide when superimposed. The diffraction patterns reveal a single diffuse peak at the angle of $2\theta = (57-59)^o$, which corresponds to the short-range order period of (0.203–0.197) nm, while there are no crystalline peaks.

The study of fractograms obtained by antiplanar deformation of the $Co_{58}Ni_{10}Fe_5Si_{11}B_{16}$ ribbons revealed a hierarchical structure in the range from 20 nm to (1–2) μm containing coral-like and cellular structures [11]. To understand the features of structure formation in AMA, it is important to note that the coral-like structure (see Fig. 1) as well as the solidification process, begins from the ribbon contact surface [12]. From the point of view of structure formation of a melt-spun ribbon as a whole, coral branches can be considered as elementary structural units of wave-like heat transfer through the ribbon thickness by means of a density gradient in the mesoscale structure. The hierarchical nature of the coral-like structure implies its quantitative parametrization by fractal dimensions.

a) *b*) *c*)

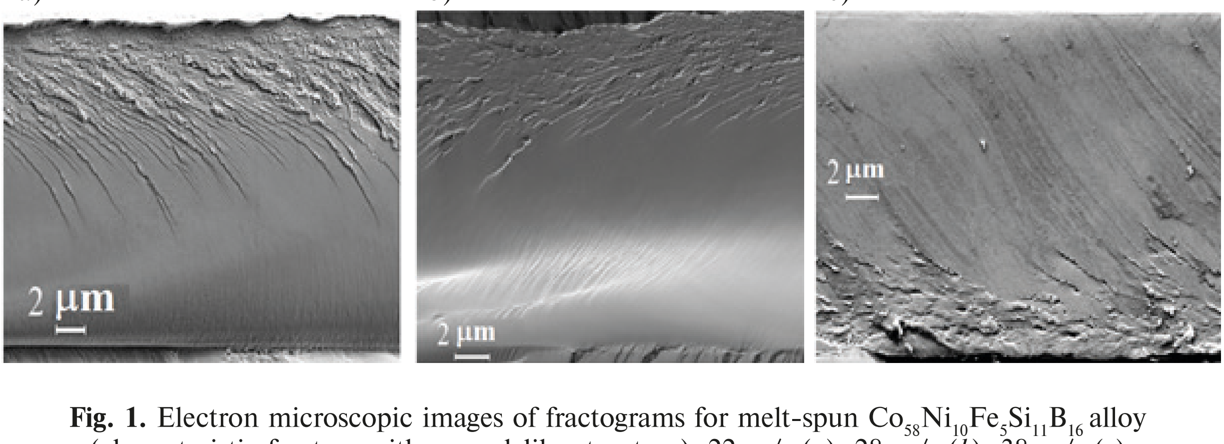

Fig. 1. Electron microscopic images of fractograms for melt-spun $Co_{58}Ni_{10}Fe_5Si_{11}B_{16}$ alloy (characteristic fracture with a coral-like structure): 22 m/s (*a*); 28 m/s (*b*); 38 m/s (*c*)

Fig. 2,*a* shows a fragment of a HRTEM image of the mesoscale structure for the sample *A*. As seen from Fig. 2,*a*, a salt-pepper contrast nanostructure is observed, typical for the amorphous structure observed in TEM images for the as-spun $Co_{58}Ni_{10}Fe_5Si_{11}B_{16}$ ribbon. We applied the fracton technique for analyzing structural ordering [7] to HRTEM images, plotting the dependence D_f(V), see Fig. 3, curve *1*. According to the kinetics of fractal dimensions, two classes of

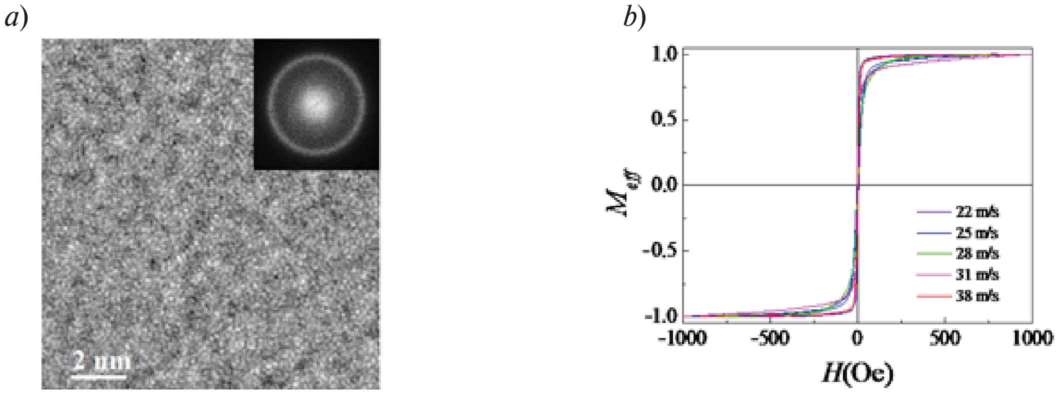

Fig. 2. HRTEM subimage of the $Co_{58}Ni_{10}Fe_5Si_{11}B_{16}$ alloy (Sample A); the inset shows the Fraunhofer diffraction pattern (*a*); hysteresis loops of the melt-spun $Co_{58}Ni_{10}Fe_5Si_{11}B_{16}$ alloy are shown in (*b*)

hierarchical subordination were distinguished by fractal dimensions greater than and less than 2. In the case of $D > 2$, the fractal cluster is the so-called contact cluster that fills the surface, for example, a fractal sponge and fractal foam [5]. Thus, the condition for the formation of a connected spatial cluster is $D > D_T = 2$.

As noted above, structure formation in AMAs affects their functional properties, in our case, magnetic ones. Therefore, it is of interest to analyze the influence of the fractal structure on the magnetic ordering. Hysteresis loops were measured for all $Co_{58}Ni_{10}Fe_5Si_{11}B_{16}$ ribbons produced at different melt-spinning conditions, Fig. 2,*b*. As seen from Fig. 2,*b,* all samples are soft magnetic. In Fig. 3, curve 2 the dependence of the coercive force (H_c) on the high-speed nonequilibrium is present. The shape of the dependence H_c(V) may be interpreted as structural relaxation within the amorphous state, accompanied by a change in the magnetic ordering.

As seen from curve *1* in Fig. 3, a fractal structure is formed in all alloys, which may be interpreted as a fractal percolation σ-cluster near a percolation threshold. However, the condition $D > 2$ is satisfied by only sample *C* (28 m/s), which implies that in this case the deterministic component prevails in the subordination by means of forming a connected spatial percolation cluster, which ensures the minimum coercive force. In cases of $D < 2$, the stochastic component dominates in the subordination; as a result, a frustrated fractal cluster is formed, which weakens largely the magnetic interaction, increasing the coercive force of these alloys.

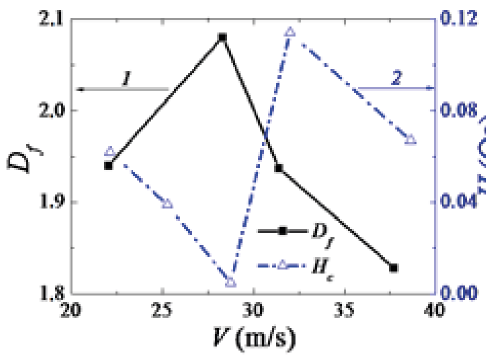

Fig. 3. Dependences of fractal dimension and coercive force for melt-spun $Co_{58}Ni_{10}Fe_5Si_{11}B_{16}$ alloy on cooling roller speed

The H_c decrease in the speed range of 22–28 m/s can be associated with an ordering change of the hierarchical complex structure of mesoscale morphological inhomogeneities due to the appearance of order from chaos (the formation of fractal dissipative structures). Moreover, with an increase of nonequilibrium, the fractal structure becomes more organized.

The amorphous state of the $Co_{58}Ni_{10}Fe_5Si_{11}B_{16}$ alloy, produced at a low speed of 22 m/s, is usually interpreted as microcrystalline, which is characterized by the presence of grain boundaries, which significantly weaken the magnetic interaction. As the cooling roller speed increases to 25 m/s, the alloy structure evolves into a heterogeneous amorphous state, while H_c decreases, identifying an increase of the magnetic interaction. These changes are due to the absence of grain boundaries in the amorphous matrix, on the one hand, and the formation of a more ordered fractal cluster (including magnetic), as a result of emergence of order from chaos, on the other hand. It is possible that the fractal cluster is still frustrated at 25 m/s due to heterogeneity of the amorphous state.

A subsequent increase of the cooling roller speed to 28 m/s results in the so-called nanocrystallization of the melt, when the nanoclusters are dissolved in an amorphous (glassy) matrix, which provides the continuity of the magnetic interaction. Thus, at optimal subordination of the multiscale structure, a minimum of the coercive force is achieved. A high value of $D_f = 2.08$ and a low value of $H_c = 0.008$ Oe indicate that a connected spatial magnetic percolation cluster is formed under these melt-spinning conditions in the amorphous matrix in addition (dualism) to the fractal cluster of morpho-inhomogeneities. In this case, it can be concluded that fractally ordered magnetic nanocrystals dissolve in an amorphous (glassy) matrix [4].

The maximum D_f is due to fractal ordering of the hierarchical complex structure of the morphological inhomogeneities of the alloy. The subsequent decrease in D_f is explained by an increase in high-speed nonequilibrium and, therefore, by a mesoscale structure randomization.

The jump of the H_c dependence from the minimum value to the maximum (Fig. 3, curve *2*) is due to the change in the ordering of the hierarchical mesoscale structure from nanocrystalline ordering, in which nanocrystals are dissolved in an amorphous matrix, where they are fractally ordered, to a homogeneous glassy state, where the magnetic percolation cluster is strongly randomized and, as a result, contains an infinite number of non-intersecting fragments. As the speed increases to 31 m/s, structural randomization destroys the nanocrystalline component, while a magnetic percolation cluster is formed in the atomic scale, which significantly weakens the magnetic interaction, increasing the H_c to a value 0.11 Oe.

The subsequent decrease in H_c with an increase of the roller speed to 38 m/s is associated with the evolution of the coral-like structure due to a reduction in the contact time of the melt with the cooling roller surface. In this case, the coral-like (foamy) structure emerges on the ribbon contact surface (Fig. 1, *c*), since the thermo-hydrodynamic wave does not have time to overcome the ribbon thickness as the ribbon quickly tears away from the cooling roller surface. Thus, the high speed results in strong randomization of the hierarchical mesoscale structure as a whole. The structure randomization is reflected by low D_f (Fig. 3, curve *1*). The short-time contact causes a heat transfer rate (supercooling degree) to decrease at such high-speed conditions, as a result, the solidification process continues after the ribbon separates from the cooling roller surface. In these conditions, magnetic nanocrystals (nanoclusters) are again formed in the glassy matrix, but they are strongly randomized and spatially broken, which follows from the reduction in the fractal dimension. It can be assumed that in the case of sample *C*, a fractal percolation cluster parameterized by $D > 2$ is formed as a result of dynamic chaos, while in other cases, with $D < 2$, the organization of structural ordering decreases as a result of the contribution from orthodox stochastization to the heat transfer process. It is likely that the high-speed conditions in which the solidification process continues outside the roller surface require taking into account the local magnetization inside the magnetic percolation cluster. Then the decrease in the coercive force of the sample *E* can be interpreted as an increase in the magnetization of non-intersecting fragments of the magnetic percolation cluster.

Based on the obtained results, it can be assumed that the hierarchical mesoscale structure of morphological inhomogeneities, characterized by fractal dimension as a randomization measure induced by high-speed nonequilibrium, determines the division of the functional space, in our case, it is the spatial distribution of the magnetic percolation cluster (ignoring magnetization), starting from short-range order scales (atomic scales) to the hierarchical (nano) cluster structure. The spatial division of both the morphological and magnetic structure is fractal (dualism), but not identical, since the obtained fractal characteristics of the hierarchical mesoscale structure of rapidly quenched $Co_{58}Ni_{10}Fe_5Si_{11}B_{16}$ alloy agree with their magnetic parameters only taking into account the difference in the structural-phase composition of the disordered material. Therefore, the fractally ordered hierarchical mesoscale structure of the ribbons determines only the nature of the magnetic division, disregarding the distribution of the magnetization magnitude. Most likely, high-speed melt-spinning processes are characterized by an increase of the randomization measure, which reduces the fractal dimensionality, on the one hand. On the other hand, an increase in the magnetization of elementary nanoclusters results in an increase in the magnetic interaction of these structures. That is, a magnetic percolation cluster must in addition be characterized by the magnetization magnitude. We can only be certain that the fractally ordered hierarchical mesoscale structure of the rapidly quenched alloy with a fractal dimension $D > 2$ provides an increase in the magnetic interaction. In this case, the $Co_{58}Ni_{10}Fe_5Si_{11}B_{16}$ alloy will have more pronounced soft magnetic properties. Thus, to obtain soft-magnetic materials, it is necessary to form an alloy structure with the maximum fractal dimension, at least in the mesoscale range.

It should be noted that the correlation between the fractal morphological structure and magnetic behaviors has a more complex dependence than that determined in the present study. It is known [8] that a dimension of the magnetic microstructure depends very strongly on the applied magnetization field. For example, the dipole-dipole interaction between nanoparticles of a fractal magnetic cluster will have a significant effect, both in low and in high fields.

Conclusion

In this work, a systematic analysis of the structural and magnetic properties of the melt-spun $Co_{58}Ni_{10}Fe_5Si_{11}B_{16}$ alloy fabricated at different melt-spinning speeds has been carried out. High-speed nonequilibrium (in the speed range V = 22–38 m/s) leads to amorphization of the alloy at all melt-spinning speed conditions, however, the structural disorder in these alloys differs largely. It is shown that the amount of order-disorder in an amorphous medium can be characterized by fractal dimension. The maximum fractal dimension is due to the fractal ordering of the hierarchical complex structure of morphological inhomogeneities into a connected spatial percolation cluster, which ensures a minimum coercive force. Thus, study of the functional properties of melt-spun alloys using fractal analysis increases the efficiency of developing technical conditions for the formation of soft magnetic materials.

Acknowledgments

The experimental results were obtained on the equipment of the Center of Collective Usage of the Far Eastern Federal University, registration No. 200556 (Vladivostok).

REFERENCES

1. **Hawelek L., Warsk T., Wlodarczyk P., Polak M., Zackiewicz P., Maziarz W., Wojcik A., Steczkowska-Kempka M., Kolano-Burian A.,** The structure and magnetic properties of rapidly quenched Fe72Ni8Nb4Si2B14 alloy, Materials. 14(1) (2021) 5–9.

2. **Han Y., Ding J., Kong F.L., Inoue A., Zhu S.L., Wang Z., Shalaan E., Al-Marzouki F.,** FeCo-based soft magnetic alloys with high Bs approaching 1.75 T and good bending ductility, Journal of Alloys and Compounds. 691 (2017) 364–368.

3. **Liu C., Inoue A., Kong F.L., Zanaeva E., Bazlov A., Churyumov A., Zhu S.L., Al-Marzouki F., Shull R.D.,** Fe-B-Si-C-Cu amorphous and nanocrystalline alloys with ultrahigh hardness and enhanced soft magnetic properties, Journal of Non-Crystalline Solids. 554 (2021) 120606.

4. **Herzer G.,** Modern soft magnets: Amorphous and nanocrystalline materials, Acta Materialia. 61(3) (2013) 718–734.

5. **Mandelbrot B.B.,** The fractal geometry of nature, Freeman, New York, 1982.

6. **Schroeder M.,** Fractals, chaos, power laws, Freeman, New York, 1991.

7. **Pisarenko T.A., Frolov A.M., Kraynova G.S.,** Evolution of structure-scaling and magnetic properties during thermal loading of melt-spun Fe70Cr15B15(Sn) alloys, Solid State Phenomena. 215 (2014) 190–195.

8. **Komogortsev S.V., Iskhakov R.S., Fel'k V.A.,** Fractal dimension effect on the magnetization curves of exchange-coupled clusters of magnetic nanoparticles, Journal of Experimental and Theoretical Physics. 128(5) (2019) 754–760.

9. **Kotvitckii A.N., Krainova G.S., Frolov A.M., Pechnikov V.S.,** Changes in the magnetic parameters of amorphous alloys as an indicator of structural transformations, Bulletin of the Russian Academy of Sciences: Physics. 77(10) (2013) 1206–1209.

10. **Grudin B.N., Plotnikov V.S.,** Processing and simulating of microscopic images, Dal'nauka, Vladivostok, 2010.

11. **Pustovalov E.V., Modin E.B., Frolov A.M., et.al.,** Effect of the process conditions for the preparation of CoNiFeSiB amorphous alloys on their structure and properties, Journal of Surface Investigation: X-ray, Synchrotron and Neutron Techniques. 13(4) (2019) 600–608.

12. **Pisarenko T.A., Kraynova G.S., Frolov A.M.,** Kinetics of the fractal mesodefect structure of melt-spun Fe70Cr15B15(Sn) alloys during annealing, Solid State Phenomena. 247 (2016) 101–105.

THE AUTHORS

FROLOV Anatoly M.
froloff5@yandex.ru
ORCID: 0000-0003-0162-6278

ILIN Nikita V.
ilin.nva@dvfu.ru
ORCID: 0000-0002-8835-6436

PISARENKO Tatiana T.A.
tata_dvo@iacp.dvo.ru
ORCID: 0000-0002-7977-7474

RALIN Andrey Yu.
ralin.ayu@dvfu.ru
ORCID: 0000-0001-6723-7246

KRAYNOVA Galina G. S.
kraynova.gs@dvfu.ru
ORCID: 0000-0001-9344-3983

Received 12.05.2022. Approved after reviewing 14.06.2022. Accepted 14.06.2022.